Statistical Analysis of Ambiguity to Signal Ratio Levels based on Global Backscattering Maps

Thomas Börner(*), Thomas.Boerner@dlr.de, +49-8153-28-2368
Mariantonietta Zonno(*), Mariantonietta.Zonno@dlr.de
Paco López-Dekker(*), Francisco.LopezDekker@dlr.de
Steffen Wollstadt(*), Steffen.Wollstadt@dlr.de
Sigurd Huber(*), Sigurd.Huber@dlr.de
Marwan Younis(*), Marwan.Younis@dlr.de
(*) German Aerospace Center, Microwaves and Radar Institute, Münchner Straße 20, 82234 Weßling, Germany

Abstract

Ambiguities are one of the limiting factors of SAR product quality and are thus important subject to every mission performance analysis. Since target NRCS is highly heterogeneous, the resulting ambiguities affect different areas at very different levels. Therefore using global average ambiguity levels for product performance assessment is of limited use. In this paper we present a statistical analysis of signal to ambiguity levels taking into account the spatial variability of the NRCS by exploiting global backscattering maps.

1 Introduction

Together with the Noise Equivalent Sigma Zero (NESZ) and single-look range and azimuth resolutions, the Range and Azimuth Ambiguity to Signal Ratios (RASR and AASR) are a two of the most relevant performance parameters characterizing a Synthetic Aperture Radar (SAR) system. The computation of these ambiguity to signal ratios take into consideration the antenna patterns, the Pulse Repetition Frequency (PRF), processing parameters (such as any applied windowing), and a backscattering profile [1]. While different profiles may be used, they include only a polarization and incidence angle dependence, both of which are only relevant for range ambiguities. The backscattering profiles represent estimates of the expected value of the Normalized Radar Cross Section (NRCS, or σ_0), so that the resulting ambiguities must be interpreted as average values.

From the observation of any SAR image it is evident that the NRCS is highly heterogeneous, so that average ambiguity levels say relatively little about the impact of ambiguities on a particular area. Thus, using them to predict final product-level mission performances is of limited use. Since, in general, the relation between product-level performance and ambiguity levels will be non-linear, average ambiguity levels do not even lead to correct average product performances.

In the work presented in this paper we study signal to ambiguity levels taking into consideration the spatial variability of the NRCS. As input we exploit global backscattering maps, which are currently available at L-, C- and X-band. Instead of considering all range or azimuth ambiguities together, like commonly done, we calculate the ambiguity rejection level for each of the most relevant range and azimuth ambiguities. The relative position of the ambiguities can be calculated using the observation geometry and PRF. Known the NRCS at the imaged point and at the ambiguities locations, ambiguity maps are generated and used for a statistical analysis.

Not only is this analysis relevant for an improved derivation of product performances, but moreover important for later application in detailed mission operation. A lot of effort is being put into the suppression of ambiguities to increase product quality [2][3], and thus precise knowledge about the expected position and level of ambiguities w.r.t. instrument, mode and mission parameters on the entire globe is a big asset.

2 Preliminary Results

In this section some preliminary results are shown. They have been obtained employing the global ALOS PALSAR backscattering maps at L-band, in HH polarization, defined on a latitude/longitude grid with a resolution of 10 arc seconds. It also includes the local topography and is available for an incidence angle of 38 degrees. Being λ the system wavelength and v the satellite velocity, the position at which the azimuth ambiguities lie with respect to a reference point at slant range distance R, is:

$$\Delta_{az} \approx \pm \frac{\lambda \cdot R \cdot PRF}{2 \cdot v} \quad (1)$$

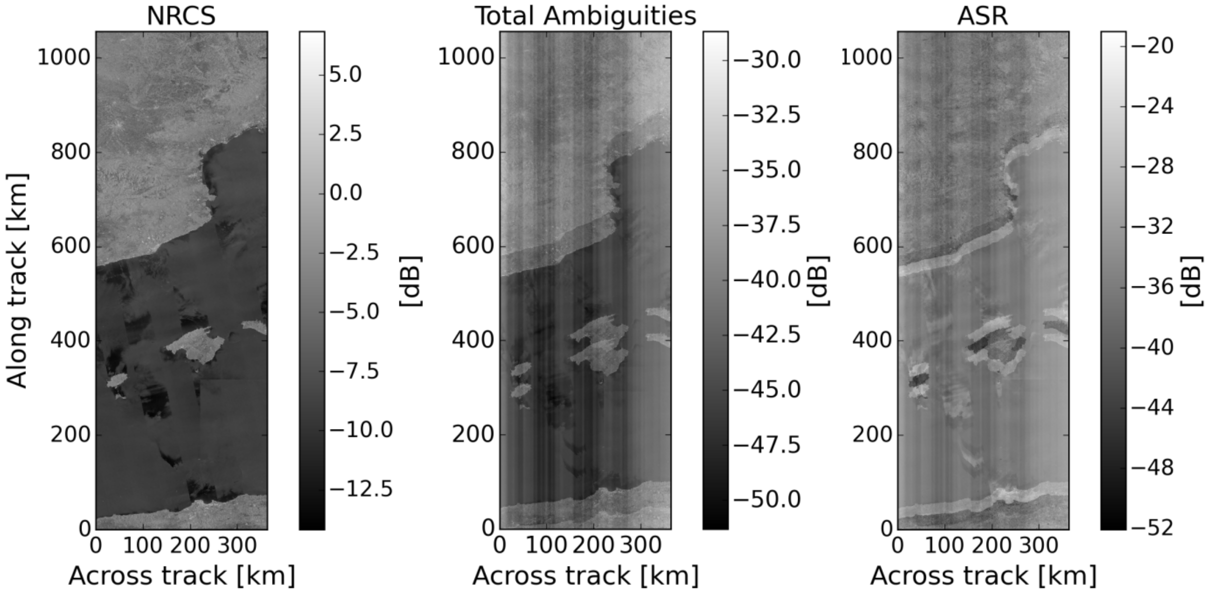

Figure 1: Backscatter and ambiguity maps over an area around Barcelona / Mediterranean Sea. Left: NRCS map derived from the global ALOS PALSAR backscattering map at L-band; middle: total azimuth ambiguities taking into account the range AASR profile; right: Azimuth Ambiguity-to-Signal Ratio (AASR).

To a first approximation, the flight direction is assumed parallel to the longitude lines of the grid: with this hypothesis the azimuth shift corresponds to a shift in latitude.

In order to compute the distance of the ambiguities Δ_{az} for every slant range distance, some of the standard Tandem-L [4] parameters, such as 24 centimeters wavelength, a PRF of 1600 Hz and an orbit height of 745 km with a velocity of almost 7.500 km/s have been used.

Known the ambiguities locations, the Azimuth Ambiguity-to-Signal Ratio (AASR) for every range line in the scene and the NRCS (see Figure 1, left), the total azimuth ambiguity map is generated as the sum of the azimuth ambiguities determined for positive and negative shifts (see Figure 1, middle). From these, the Azimuth Ambiguity-to-Signal Ratio (AASR) can be determined (see Figure 1, right).

As a first approach to statistical analysis we compute the histograms of the “products” shown in Figure 1. As expected from the land/sea scenario the NRCS histogram is clearly bimodal (see Figure 2). Since the total azimuth ambiguities consist of positive and negative shifts based on the original NRCS in combination with range variability, the histogram is still bimodal, but blurred (see Figure 3). Even more interesting is the histogram of the AASR, still showing bimodal behavior, however, this time not clearly related to land- or sea-areas, but moreover related to the land/sea boundary (coastline), where the ratio of bright land scattering to lower sea scattering becomes apparent (see Figure 4).

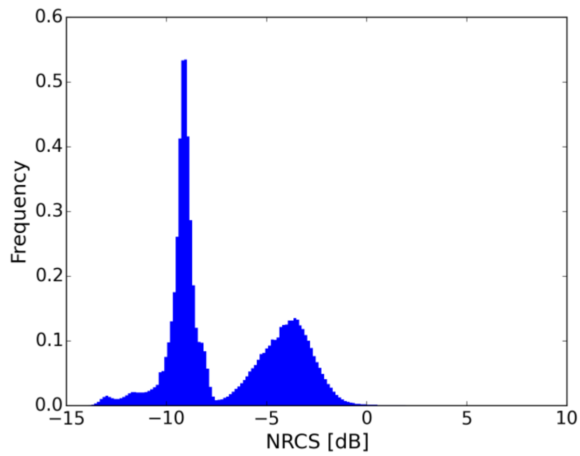

Figure 2: Histogram of the NRCS shown in Fig. 1 left.

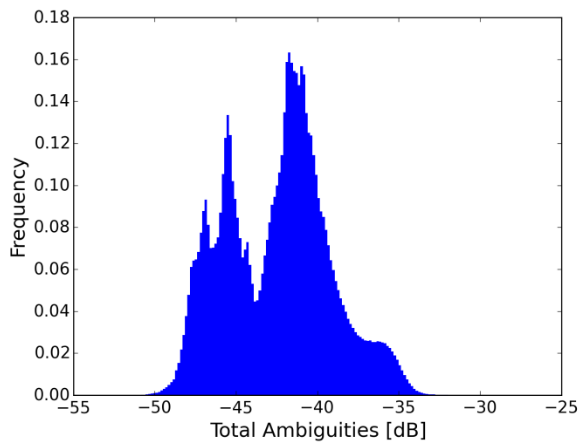

Figure 3: Histogram of the total ambiguities shown in Fig. 1 middle.

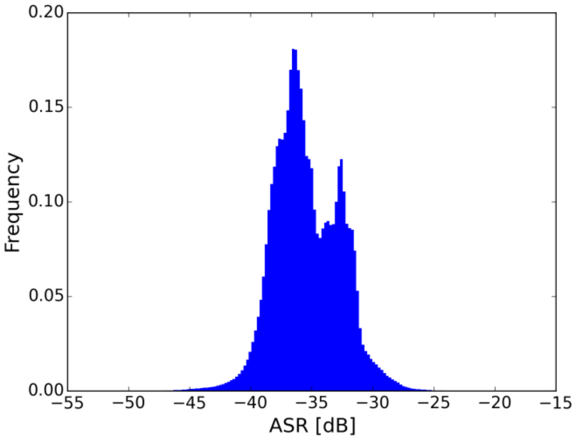

Figure 4: Histogram of the AASR shown in Fig. 1 right.

Currently the main output of these histograms is the amount of resolution cells or map/product area which is subject to corruption by ambiguities, e.g. where the AASR exceeds a defined threshold. This threshold will depend on user- and system-requirements and could be somewhere in the range of -30 to -20 dB (e.g. ERS-1 is marked as excellent at azimuth ambiguity levels of around -28 dB [5]). For instance, in our actual scenario the AASR histogram yields that only very few pixels exceed -25 dB, and thus that this map/product may be flagged as “unaffected by ambiguities” w.r.t. the chosen threshold.

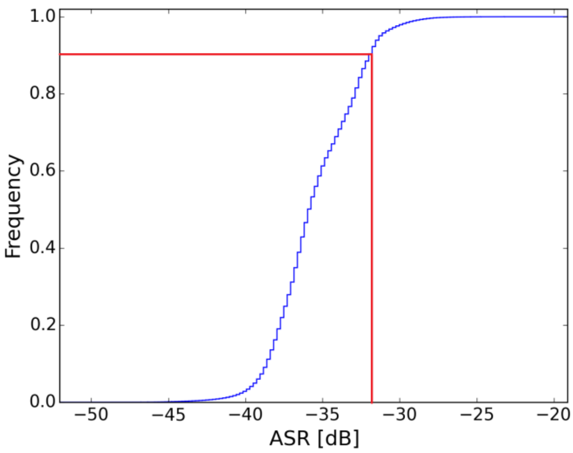

Figure 5: Cumulative density function (blue line) of the AASR histogram shown in Fig. 4. The red line depicts the AASR at 90% probability, which corresponds to an AASR of -32 dB.

Area-wise derived AASR histograms can furtherly be exploited for a mission-wide (global) statistical analysis by computing the Cumulative Density Function (CDF), as shown in Figure 5. From this it can easily be derived that for example 90% of all samples have an AASR below -32 dB. The AASR threshold as well as the minimum amount of samples below this threshold (via the CDF) are then two parameters, which can be chosen by the user to flag areas subject to possible corruption by ambiguities.

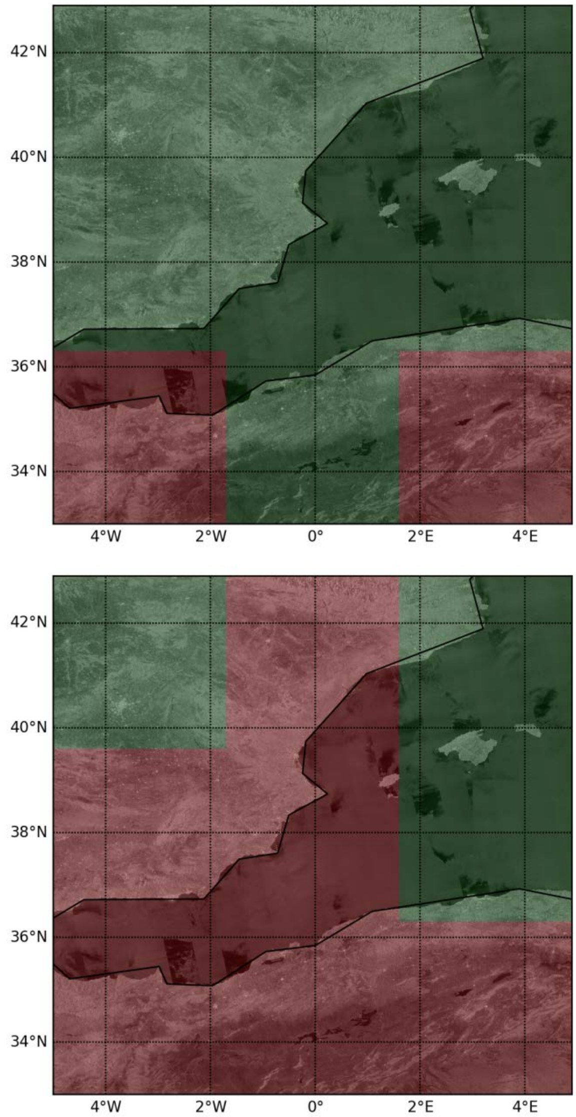

Figure 6: Exemplary azimuth ambiguity performance map. $AASR_{th}$ = -30 dB; top: PIX_{th} = 97.0%; bottom: PIX_{th} = 97.5%. Green patches meet the set conditions, whereas red patches do not.

As a first attempt towards a global performance map w.r.t. azimuth ambiguities, the following exemplary experiment has been carried out: 9 neighboring patches of data from the global backscattering map have been chosen such that they cover the area from 33° to 43° latitude and from -5° to +5° longitude, each patch being approximately 350 km x 350 km in size. For each of these patches the AASR is derived and the cumulative density function is calculated. The CDF is then analyzed whether it meets predefined thresholds or not. The ASR threshold $AASR_{th}$ is set to -30 dB. For the minimum amount of pixels below $AASR_{th}$ the CDF is tested against a percentage of PIX_{th} = 97.0% and PIX_{th} = 97.5%, respectively. The results are shown in Figure 6, i.e. maps with green and red patches, where the green ones meet the conditions. Red flagged patches would be candidates for e.g. application of ambiguity suppression techniques.

Note that the threshold levels in the previous example are neither realistic nor reasonable w.r.t. the used Tandem-L mission parameters. They have been merely chosen to visualize and demonstrate a possible result for a mission-wide global performance analysis.

3 Conclusions and Outlook

The preliminary results of section 2 already show the advantageous approach of a statistical analysis of ambiguities, since areas affected by too strong ambiguities (the AASR exceeding a certain level) can be identified in advance. However, statistics will certainly be capable of revealing much more information, which will be the subject of future studies.

We intend to analyze also the statistics of range ambiguities (RASR) and the impact on global performance. Furthermore we seek for a more realistic implementation, i.e. considering real orbits and more detailed mission- and system- parameters, which was started but not finished at the time of the paper deadline.

References

[1] Mirko P. Zénere, University Cordoba, http://aulavirtual.ig.conae.gov.ar/moodle/pluginfplu.php/513/mod_page/content/78/MirkoPanozzoMirkoP.pdf, Final Seminar Report, 2012.

[2] Federica Bordoni, Marwan Younis, Gerhard Krieger, *Ambiguity Suppression by Azimuth Phase Coding in Multichannel SAR Systems*, IEEE Trans. Geosc. and Remote Sensing, vol. 50, no. 2, pp. 617-629, 2012.

[3] Andrea Monti Guarnieri, *Adaptive Removal of Azimuth Ambiguities in SAR Images*, IEEE Trans. Geosc. and Remote Sensing, vol. 43, no. 3, pp. 625-633, 2005.

[4] Marwan Younis, Sigurd Huber, Carolina Tienda Herrero, Gerhard Krieger, Alberto Moreira, Akihisa Uematsu, Yasuo Sudo, Ryoko Nakamura, Yoshikazu Chishiki, Masanobu Shimada, *Tandem-L Instrument Design and SAR Performance Overview*, Proc. IGARSS, Québec City, Canada, 2014.

[5] Peter J. Meadows, H. Laur, Betlem Rosich, Birgit Schättler, *The ERS-1 SAR Performance: A Final Update*, Proc. CEOS SAR Workshop, Tokyo, Japan, April 2001.